

Facile Construction of Mesoporous N-Doped Carbons as Highly Efficient 4-Nitrophenol Reduction Catalysts

Ying Yang,* Wen Zhang, Xiaohui Ma, Hairui Zhao, and Xin Zhang*^[a]

Herein we propose a novel *in situ* N-doping method to develop a new type of mesoporous N-doped carbons constructed by direct pyrolysis of properly rigid strut N-rich metal–organic frameworks at 950 °C. This facile fabrication method creates doped N that is evenly dispersed on mesoporous carbons (≈ 4.0 nm) formed simultaneously without the need for a second carbon precursor, external nitrogen supplier, or pore-forming agent. The resulting mesoporous N-doped carbons bear a low N content but a high proportion of graphitic N species and exhibit superior catalytic performance toward the reduction of 4-nitrophenol relative to that shown by previously reported metal catalysts and N-doped graphene. The ensemble effect of the mesostructured framework and effective N doping is responsible for the excellent performance, as better diffusion, adsorption, and activation of 4-nitrophenol in wastewaters are achieved through the elaborately fabricated mesoporous N-doped carbons.

The design and application of N-doped carbons has become a hot topic, as N doping has proven to be a powerful method to modify the properties of carbon materials and thus provides a promising way to extend the applications of such materials from adsorption, energy conversion, and storage to catalysis. Various metal-free gas sensors,^[1] supercapacitors,^[2] electrochemical oxygen reduction reaction catalysts,^[3] and metal-free oxidative^[4] and basic^[5] catalysts have been developed by doping N into carbons either directly during synthesis or by postsynthetic treatment. Postsynthetic treatment of carbon materials often leads to less-efficient surface functionalization; in contrast, doping of carbons during synthesis by using N-containing precursors (*in situ* N doping) can realize the homogeneous incorporation of nitrogen into the entire carbon materials, which facilitates control of the nitrogen dosage and dopant state.^[6] Indeed, N-doped carbon nanotubes and carbon nanofibers have been synthesized by methods similar to those used to prepare bulk carbon nanotubes by using precursors such as melamine,^[7] acetonitrile,^[8] nitrogen heterocycles,^[9] and phthalocyanines.^[10] Notably, such N-doped carbons often bear low accessible surface areas and microporosities owing to the absence of a well-defined precursor structure, which inevitably

erodes substrate diffusion and mass transfer. On the other hand, mesoporous N-doped carbons (MNCs) with large surface areas and regularly arranged mesopores were first developed by a hard-templating approach, which involves filling the mesoporous silicate pores with nitrogen and carbon suppliers followed by carbonization and final silicate template removal.^[11] Alternatively, by using an extra N supplier, the soft-templating method can be made more step economical for the construction of MNCs simply by direct pyrolysis of well-defined C,N-containing supramolecular aggregates.^[12] However, the generality of this methodology is doubtful, because the harmonious interaction between precursors and surfactant is crucial to mesostructure formation, which decides the final porosity, and thereby the available N suppliers are quite limited. Despite continuous efforts, the facile and large-scale fabrication of MNCs still remains a challenge.

Currently, metal–organic frameworks (MOFs) as a novel class of nanoporous crystalline materials built from transition-metal clusters as nodes and organic ligands as struts act as both templates and precursors for the preparation of porous carbon materials.^[13] Owing to the large carbon content in MOFs, nanoporous carbons (NPCs) also can be achieved by direct carbonization of MOFs without the need for any additional carbon source. Thus, several Zn-containing MOFs, such as ZIF-8, ZnBTC, and the isoreticular metal–organic framework series, IRMOF-*x* (*x* = 1, 3, and 8), are used as the sole carbon precursors to yield highly porous nanocarbons with ultrahigh surface areas that show excellent properties in gas adsorption, electrochemical capacitance, sensing, and catalysis.^[14] However, these NPCs always possess a broad pore-size distribution, probably because pyrolysis at low temperature (≤ 800 °C) followed by acid washing erodes the pore arrangement upon ZnO removal. Subsequently, the one-pot conversion of zinc–dicarboxylic acid containing MOFs at high temperature (950 °C) was recently proven by us to be effective in obtaining narrowly distributed mesopores by vaporizing away Zn metal (b.p. 908 °C) during pyrolysis.^[15] Inspired by this, the incorporation of nitrogen into a similar zinc–dicarboxylic acid constructed MOF precursor could facilitate the one-pot synthesis of MNCs after pyrolysis at 950 °C.

To realize efficient N doping into the mesoporous carbons by direct pyrolysis of zinc–dicarboxylic acid containing MOFs, we hypothesized that such MOF precursors should be properly rigid and bear a large amount of evenly distributed N moieties as the component of the organic struts on the basis of the following considerations:

- 1) A MOF precursor having a properly rigid crystalline structure can afford regular mesostructures after pyrolysis. Oth-

[a] Dr. Y. Yang, Dr. W. Zhang, Dr. X. Ma, Dr. H. Zhao, Prof. X. Zhang
China University of Petroleum
State Key Laboratory of Heavy Oil Processing
No.18, Fuxue Road, Changping District, Beijing 102249 (P.R. China)
E-mail: catalyticsscience@163.com
zhangxin@cup.edu.cn

Supporting Information for this article is available on the WWW under <http://dx.doi.org/10.1002/cctc.201500807>.

erwise, only randomly distributed pores are derived from flexible MOFs, or mere regular micropores are produced from rigid MOFs.

- 2) Carbonization at high temperature requires sufficient and stable N species to be introduced to guarantee the proper N dosage in the final state. Though the component N species from the organic struts is in excess, they could be mostly converted into volatile species during pyrolysis, let alone the loosely attached N moieties, which could vaporize away completely upon heating at 950 °C. In this sense, MNCs could be facily constructed by direct pyrolysis of properly rigid strut N-rich MOFs.

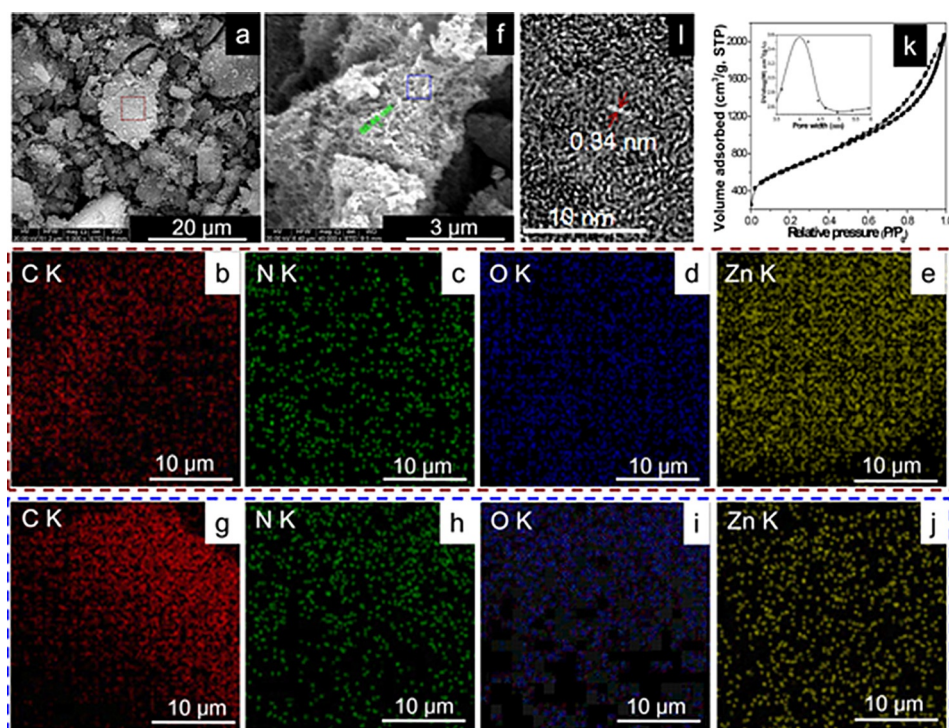


Figure 1. Characterization of the NZnMOF precursor and MNC: a) SEM image of NZnMOF; b–e) C, N, O, and Zn elemental maps of NZnMOF; f) SEM image of MNC; g–j) C, N, O, and Zn elemental maps of MNC; k) N₂ adsorption/desorption isotherm and the corresponding pore-size distribution curve of MNC (inset); and l) high-resolution TEM image of MNC.

To verify this hypothesis, we designed a properly rigid MOF precursor constructed with zinc clusters and inexpensive acidic α -diamine struts, 1,4-bis(4-CO₂HC₆H₄)-2,3-dimethyl-1,4-diazabutadiene, which was facily synthesized by the condensation of 4-aminobenzoic acid with 2,3-butanedione by using formic acid as the catalyst (Scheme 1 a; see also Figures S1 and S2, Supporting Information).^[16] The resulting N-rich zinc-dicarboxylic acid containing MOF (NZnMOF, see Figure S3a) is well crystalline (Figure S4a) and has a stone-like morphology (Figure 1 a); furthermore, it displays a uniform distribution of the C, N, O, and Zn elements, as determined by X-ray diffraction (XRD), scanning electron microscopy (SEM), energy-dispersive X-ray spectroscopy (EDX) (Figure S5 a), and SEM mapping results (Figure 1 b–e). The MNC was subsequently obtained by direct pyrolysis of NZnMOF under a N₂ atmosphere at 950 °C for 2 h (Scheme 1 b), which yielded fluffy and highly porous carbons (Figure 1 f) with an even distribution of inserted N upon Zn removal (Figure 1 g–j and Figure S5 b) and bearing a mesoporous structure and a narrow mesopore size

distribution centered at approximately 4.0 nm (Figure 1 k). The high-resolution transmission electron microscopy (TEM) image shows that the interplane spacing of the (002) crystal lattice is approximately 0.34 nm (Figure 1 l), in agreement with the interlayer distance of graphite.^[17] The XRD pattern displays (002) and (10 1) diffraction peaks at $2\theta = 26$ and 43° , respectively (Figure S4 b), which is suggestive of a well-defined graphitic structure.^[17] These results demonstrate that the MNCs can be facily fabricated by one-pot conversion of properly rigid strut N-rich MOFs at high temperature.

The use of N-doped carbons for sewage treatment is highly desirable, as highly efficient catalysts with a low cost and high stability are urgently required for the large-scale degradation of organic pollutants generated from agricultural and industrial sources. Among which, the catalytic reduction of 4-nitrophenol (4-NP) is of great importance, because it makes waste profitable owing to the production of industrially related 4-aminophenol (4-AP) as a source for the production of aniline and paracetamol.^[18] For this process, various supported metal catalysts, such as Au, Pd, Ag, and Ni, and bimetallic catalysts, such as PtNi, AuCu, and PdCu,^[19] have been proven to be highly active for the conversion of 4-NP. Metal-free catalysts have recently emerged as new and promising candidates for the reduction of 4-NP. Gazi and Ananthakrishnan reported the metal-free-photocatalytic reduction of 4-NP by using a resin-supported dye under visible-light irradiation.^[20] More recently, N-doped graphene (NG) was found to be active toward the reduction of 4-NP and exhibited activity comparable to that of



Scheme 1. Schematic illustration of a) the synthesis of 1,4-bis(4-CO₂HC₆H₄)-2,3-dimethyl-1,4-diazabutadiene (L) and b) the synthesis of mesoporous N-doped carbons through pyrolysis of N-rich MOF precursors.

metal catalysts.^[21] In our experiment, NaBH₄ was not able to reduce 4-NP even after 2 days without a catalyst. However, with an ultrasmall amount of added MNC, the color of the reaction mixture changed from yellow to entirely colorless after 10 min (Figure 2a). Considering the possibility that there could be a decrease in the concentration of 4-NP caused by the adsorption of 4-NP on the large surface area of the MNC, a control experiment was undertaken. 4-NP and the MNC were mixed in the presence of water, and the resultant mixture was analyzed by UV/Vis spectroscopy (Figure S6). The adsorption of 4-NP on the MNC was found to be insignificant. A significant decrease in the absorbance at $\lambda=400$ nm associated with concomitant evolution of a peak at $\lambda=298$ nm (Figure 2b) is further indicative of the reduction of 4-NP to 4-AP.^[19b] The conversion of 4-NP was calculated from Equation (1):

$$\text{Conversion [\%]} = \frac{C_t}{C_0} \quad (1)$$

in which C_0 and C_t are the concentrations of 4-NP at time t and 0, respectively, measured from the relative intensity of absorbance (A_t/A_0) at $\lambda=400$ nm. The four marked isosbestic points at $\lambda=224, 245, 281,$ and 313 nm are clear, which is demonstrative of a clean conversion process without the formation of any byproducts.^[22] GC-MS analysis also demonstrated the conversion of 4-NP into 4-AP (Figure S7).

Interestingly, the absorbance intensity at $\lambda=400$ nm and the conversion of 4-NP change linearly with time (t) for the MNC-

catalyzed reaction (Figure S8 and Figure 2c), and this is indicative of pseudo-zero-order kinetics ($k=5.8 \times 10^{-8} \text{ mol L}^{-1} \text{ s}^{-1}$), in accordance with the reaction kinetics reported for NG. The nonlinear relationship between $\ln(C_t/C_0)$ and t (Figure 2d) further demonstrates the completely different reaction kinetics from a metal-catalyzed first-order reaction,^[19] whereas the MNC shows activity that is comparable to that of previously reported metal catalysts.^[23] To compare the activities of the different N-doped carbons, the specific rate constant (K) [Eq. (2)] was then calculated:

$$K = \frac{k}{m} \quad (2)$$

in which k is the rate constant and m is the mass of the catalyst in grams.

It is clear that the MNC exhibits a much larger specific rate constant ($11.6 \times 10^{-4} \text{ mol L}^{-1} \text{ s}^{-1} \text{ g}^{-1}$) than NG ($5.3 \times 10^{-4} \text{ mol L}^{-1} \text{ s}^{-1} \text{ g}^{-1}$) (Table S1), and this suggests that the MNC has a higher activity than NG. Furthermore, the MNC can be easily recycled up to 11 times and displays high activity ($\approx 98\%$) after 7 cycles if the reaction is allowed to proceed for 10 min, and this is indicative of its superior recyclability (Figure 2e).

A question that needs addressing is what makes the MNC more efficient than NG? Thus, we conducted a series of characterizations and comparative experiments in an attempt to understand the relationship between textural properties, N status, and catalytic performance of the MNC.

In a control experiment, a similar N-doped carbon (NC) was synthesized by direct pyrolysis of N-rich zeolitic imidazolate frameworks (ZIF-8) and was comparatively studied (Supporting Information). It is surprising that the NC was completely inactive (Figure S9), even though the amount of catalyst used was increased or the reaction time was prolonged. The N₂ adsorption reveals that the NC shows a type I isotherm (Figure S10) and a high specific surface area of $1043 \text{ m}^2 \text{ g}^{-1}$ (Table 1); these are indicative of its microporous nature.^[24] Moreover, the MNC exhibits a type IV isotherm with a narrow pore-size distribution centered at approximately 4.0 nm (Figure 1k and Table 1). During the pseudo-zero-order reaction, the adsorption of 4-NP ions is much faster than desorption, so the number of 4-NP ions adsorbed on the MNC is not determined by their concentration but by the number of active sites on the MNC. In this perspective, the mesopore structure in the MNC undoubtedly facilitates diffusion of the 4-NP ions and accelerates their adsorption onto the active sites, which is linked to the superior performance. Likewise, the MNC also shows an advantage over microporous NG in terms of mass transportation, and thereby the MNC exhibits a higher reaction rate. Therefore, the pore size plays a vital role in catalytic activity by affecting mass transportation, which is in accordance with the reported role of the pore size on mass transport in proton-exchange-membrane fuel cells.^[25]

In a comparative experiment, a pure mesoporous carbon (MC) was prepared by direct pyrolysis of MOF-5 (Supporting Information); it was proven to be inactive (Figure S11), though it

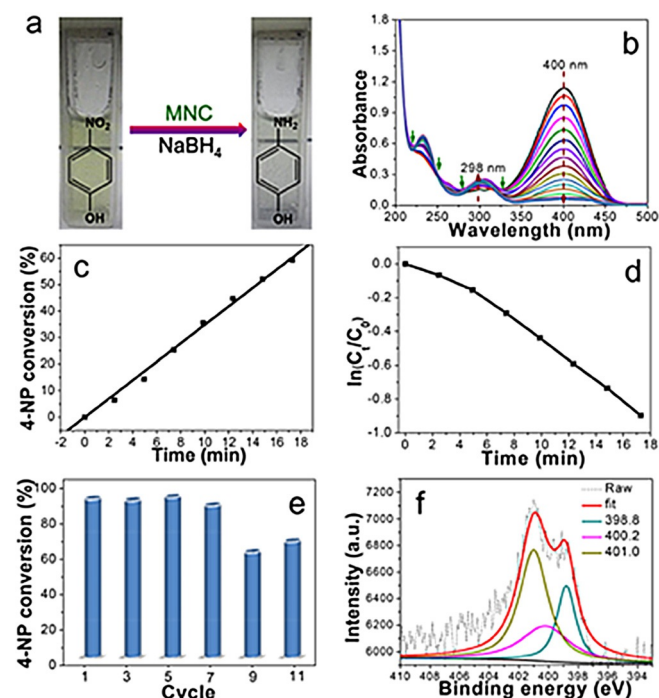


Figure 2. a) Optical photos of the color change during the reaction, b) the reduction of 4-NP in aqueous solution recorded every 2.5 min by using 0.05 mg MNC, c) time-dependent conversion of 4-NP, d) the relationship between $\ln(C_t/C_0)$ and reaction time (t), e) catalytic conversion of 4-NP at different cycles, and f) the XPS spectrum of the N 1s region for MNC.

Table 1. Textual properties and surface N content from XPS analysis.

Material	$S_{\text{BET}}^{[a]}$ [m ² g ⁻¹]	$V_p^{[b]}$ [cm ³ g ⁻¹]	$D_p^{[c]}$ [nm]	Elemental N content [wt%]	XPS N content [wt%/at%]	Different N content [at%]			
						Graphitic	Pyridinic	Pyrrodic	Amine
MNC	2269	2.813	4.0	3.6	(3.2/2.8)	50.1	23.1	26.8	–
NC	1043	0.536	nd	–	–	–	–	–	–
NG ^[d]	–	–	–	14.7	(13.0/11.1)	11.1	44.4	22.2	22.2
MC	2817	2.097	4.2	–	(0/0)	0	0	0	0
MNC-p	615	0.540	4.0	3.1	(2.4/2.1)	57.3	21.1	21.6	–

[a] The BET surface area was obtained from the adsorption branches in the relative pressure range of 0.05 to 0.20. [b] The single-point adsorption total pore volume was taken at a relative pressure of 0.99. [c] The pore-size distribution was calculated from the desorption branches by the Barret–Joyner–Halenda (BJH) method; nd = not detected. [d] Data taken from Ref. [21].

does have a high surface area of 2817 m²g⁻¹ and a mesopore size of 4.2 nm (Figure S12 and Table 1). This result is indicative of the critical role of N doping in this reaction. The MNC is active because high positive spin and asymmetric charge density are introduced by N doping, which confers quasimetallic properties onto the N-doped carbons. The total amount of N in the MNC is 3.6 wt%, and the surface N content is approximately 3.2 wt% (corresponding to 2.8 at%) estimated by X-ray photoelectron spectroscopy (XPS) analysis (Table 1), which is much lower than the corresponding N content in NG. It is clear that excessively doped N species cannot bring about high activity, which is similar to oxidative catalysis^[4b] but contrary to N-doped electrochemical^[3a] and basic catalysis.^[5] To gain deeper insight into the doped N status, the N 1s binding energies of the MNC were investigated, and the corresponding spectra were composed (Figure 2 f) and integrated (Table 1). The N 1s narrow scan spectrum was deconvoluted into three types of doped N: graphitic (401.0 eV), pyrrodic (400.2 eV), and pyridinic (398.8 eV) configurations^[26] in proportions of 23.1, 26.8, and 50.1 at%, respectively. NG also shows four types of doped N with different proportions: graphitic (401.4 eV, 11.1 at%), pyrrodic (400.2 eV, 22.2 at%), amine (399.5 eV, 22.2 at%), and pyridinic (398.6 eV, 44.4 at%) configurations.^[21] It is suggested that the activity is not dependent on the amount of doped N but on the total amount of graphitic N species that supply proper adsorption sites for the activation of 4-NP during the reaction^[21] and that are considered to be the active sites. In this study, the higher active N content (50.1 at%) can be attributed to the enhanced activity of the MNC, and it is probable that pyrolysis at a high temperature (950 °C) facilitates the conversion of amine N species into graphitic N species. If this is true, further improvement in the graphitic N content in the N-doped mesoporous carbon could bring about better activity. To verify this speculation, IRMOF-3 was chosen as a model, because it contains rich and easily converted amine N species. In our experiment, as-synthesized IRMOF-3 was directly pyrolyzed at 950 °C to yield another mesoporous N-doped carbon, that is, MNC-p (Supporting Information). XRD and N₂ adsorption studies demonstrate that its graphitic structure (Figure S13) and pore size are similar to those of the MNC (Figure S14 and Table 1). Elemental analysis revealed that the total N content in the MNC-p is approximate-

ly 3.1 wt%, and the surface N content is approximately 2.4 wt% (corresponding to 2.1 at%), as estimated by XPS analysis (Table 1), which is less than the corresponding N content in the MNC. The N 1s spectrum could also be deconvoluted into three kinds of doped N: graphitic (401.2 eV), pyrrodic (400.2 eV), and pyridinic (398.3 eV) configurations (Figure S15) with compositions of 21.1, 21.6, and 57.3 at%, respectively. It is clear that the propor-

tion of graphitic N was improved by 7.2% in the MNC-p relative to the graphitic N content in the MNC. It is speculated that the parent NH₂ moieties in IRMOF-3 can be facily converted into graphitic N species; whereas the C=N groups in N₂ZnMOF may undergo transformation from imine groups into amine groups before their conversion into graphitic N, which thus leaves fewer graphitic N species. Accordingly, the MNC-p shows a larger rate constant (6.4 × 10⁻⁸ mol L⁻¹ s⁻¹, see Figure S16 and Table S1) and a larger specific rate constant (12.7 × 10⁻⁴ mol L⁻¹ s⁻¹ g⁻¹) than the MNC and can be recycled many times (Figure S17). On the basis of these results, it is clear that the activity decreases with an increase in the elemental and XPS N content over the three N-doped carbons (Figure 3 a), which suggests that only a small amount of graphitic N is needed for this reaction. On the other hand, the activity increases with an increase in the proportion of graphitic N species (Figure 3 b), which play a significant role in the adsorption and activation of 4-NP. Therefore, the proportion of graphitic N incorporated proves to be decisive to catalytic performance, whereas a small amount of active sites are satisfied.

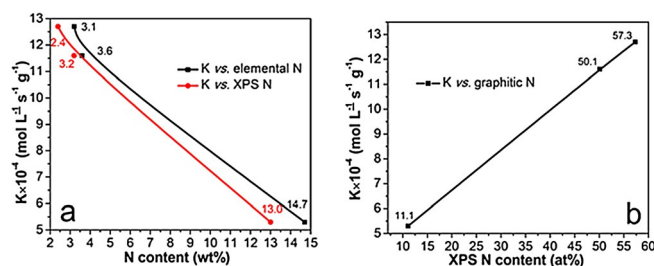


Figure 3. The relationship of specific rate constant versus a) elemental and XPS N content and b) the proportion of graphitic N species.

In summary, a new type of mesoporous N-doped carbon (MNC) was successfully developed in situ by a facile synthetic methodology: direct pyrolysis of a properly rigid strut N-rich metal–organic framework (MOF) at 950 °C. High-temperature treatment facily created a low content of N but simultaneously formed a sufficient number of active N sites evenly dispersed on the mesoporous carbons. The resulting mesoporous

N-doped carbons exhibited pseudo-zero-order kinetics toward the reduction of 4-nitrophenol and show catalytic performance that is superior to that of previously reported metal catalysts and N-doped graphene. The excellent catalytic performance can be ascribed to the ensemble effect of the elaborately designed mesostructures and the doped N sites, which facilitate diffusion of 4-nitrophenol and accelerate its adsorption and activation on the active N sites. The successful design of highly active MNCs gives a strong indication of the generality of this method for the facile construction of various mesoporous N-doped carbons through such a unique "one stone, three birds" strategy to carbonize MOFs, to convert N species, and to vaporize Zn metal in a single step. This unprecedented approach not only opens another gateway for applications of N-containing MOF but also provides new insight for N-doping strategies.

Experimental Section

Sample preparation

4-Aminobenzoic acid (57.6 g, 420 mmol) was dissolved in MeOH (200 mL) containing formic acid (80 drops) as the catalyst. Then, 2,3-butanedione (17.6 mL, 200 mmol) was added dropwise, and the resulting mixture was stirred at ambient temperature for 24 h. The resulting pale-yellow precipitate was isolated by filtration and was washed with cold methanol to afford acidic α -diimine ligand **L**. Then, zinc nitrate hexahydrate (9.0 g, 30 mmol) and **L** (3.2 g, 10 mmol) were dissolved in DMF (50 mL) under constant agitation under atmospheric conditions. Upon the formation of a clear solution, triethylamine (11 mL) was added dropwise, and the mixture was stirred for another 1 h. The resulting dark-yellow solid was filtered off, washed with DMF, and dried under vacuum to yield the nonporous NZnMOF precursor. As-made NZnMOF was placed in a quartz boat, flushing with N₂ flow, and was further heated in a horizontal tube furnace up to 950 °C at a rate of 5 °C min⁻¹ and was maintained at this temperature for 2 h under N₂ flow to yield the mesoporous N-doped carbon (MNC).

Catalytic test

The reduction of 4-nitrophenol (4-NP) was performed in a quartz cuvette and was monitored by UV/Vis spectroscopy (754PC) at room temperature. A solution of 4-NP in water (0.01 M, 25 μ L) was mixed with certain content of the catalyst in sodium borohydride aqueous solution (2.5 mL), and UV spectroscopy was employed to in situ monitor the reduction by measuring the absorbance of the solution at λ = 400 nm as a function of time at an interval of 2.5 min. After the reaction was finished, the mixture was centrifuged and washed with ethanol (3 \times) and water (3 \times). The resulting catalyst was redispersed in aqueous 4-NP solution (0.01 M, 25 μ L) and fresh NaBH₄ solution (2.5 mL), and the test was repeated to probe the stability. In this study, the linear relationships between the conversion of 4-NP and the reaction time and between the absorbance of 4-NP and the reaction time were observed, and the fitting showed R² > 0.99800 and a standard error smaller than 0.06.

Acknowledgements

The authors gratefully acknowledge financial support from the National Natural Science Foundation of China (21303229,

21173269, 91127040), Beijing Natural Science Foundation (2152025), the Science Foundation of China University of Petroleum, Beijing (2462013YJRC018), Ministry of Science and Technology of China (2011BAK15B05), and Specialized Research Fund for the Doctoral Program of Higher Education (20130007110003).

Keywords: doping • mesoporous materials • metal–organic frameworks • pyrolysis • reduction

- [1] a) M. Hamadanian, B. Khoshnevisan, F. K. Fotooh, *Struct. Chem.* **2011**, *22*, 1205–1211; b) L. Bai, Z. Zhou, *Carbon* **2007**, *45*, 2105–2110.
- [2] a) Y. S. Yun, H. H. Park, H. J. Jin, *Materials* **2012**, *5*, 1258–1266; b) K. S. Kim, S. J. Park, *J. Electroanal. Chem.* **2012**, *673*, 58–64; c) F. W. Ma, H. Zhao, L. P. Sun, Q. Li, L. H. Huo, T. Xia, S. Gao, G. S. Pang, Z. Shi, S. H. Feng, *J. Mater. Chem.* **2012**, *22*, 13464–13468.
- [3] a) T. C. Nagaiah, A. Bordoloi, M. D. Sánchez, M. Muhler, W. Schuhmann, *ChemSusChem* **2012**, *5*, 637–641; b) Z. Y. Lin, M. K. Song, Y. Ding, Y. Liu, M. L. Liu, C. P. Wong, *Phys. Chem. Chem. Phys.* **2012**, *14*, 3381–3387.
- [4] a) K. Chizari, A. Deneuve, O. Ersen, I. Florea, Y. Liu, D. Edouard, I. Janowska, D. Begin, C. Pham-Huu, *ChemSusChem* **2012**, *5*, 102–108; b) Y. J. Gao, G. Hu, J. Zhong, Z. J. Shi, Y. Zhu, D. S. Su, J. G. Wang, X. H. Bao, D. Ma, *Angew. Chem. Int. Ed.* **2013**, *52*, 2109–2113; *Angew. Chem.* **2013**, *125*, 2163–2167.
- [5] X. Jin, V. V. Balasubramanian, S. T. Selvan, D. P. Sawant, M. A. Chari, G. Q. Lu, A. Vinu, *Angew. Chem. Int. Ed.* **2009**, *48*, 7884–7887; *Angew. Chem.* **2009**, *121*, 8024–8027.
- [6] a) D. S. Su, J. Zhang, B. Frank, A. Thomas, X. C. Wang, J. Paraknowitsch, R. Schlögl, *ChemSusChem* **2010**, *3*, 169–180; b) C. H. Zhang, L. Fu, N. Liu, M. H. Liu, Y. Y. Wang, Z. F. Liu, *Adv. Mater.* **2011**, *23*, 1020–1024.
- [7] a) M. Terrones, P. Redlich, N. Grobert, S. Trasobares, W. K. Hsu, H. Terrones, Y. Q. Zhu, J. P. Hare, C. L. Reeves, A. K. Cheetham, M. Rühle, H. W. Kroto, D. R. M. Walton, *Adv. Mater.* **1999**, *11*, 655–658; b) M. Terrones, H. Terrones, N. Grobert, W. K. Hsu, Y. Q. Zhu, J. P. Hare, H. W. Kroto, D. R. M. Walton, P. Kohler-Redlich, M. Rühle, J. P. Zhang, A. K. Cheetham, *Appl. Phys. Lett.* **1999**, *75*, 3932–3934.
- [8] a) M. Glerup, M. Castignolles, M. Holzinger, G. Hug, A. Loiseau, P. Bernier, *Chem. Commun.* **2003**, 2542–2543; b) A. G. Kudashov, A. V. Okotrub, L. G. Bulusheva, L. P. Asanov, Y. V. Shubin, N. F. Yudanov, L. I. Yudanov, V. S. Danilovich, O. G. Abrosimov, *J. Phys. Chem. B* **2004**, *108*, 9048–9053.
- [9] a) R. Sen, B. C. Satishkumar, S. Govindaraj, K. R. Harikumar, M. K. Renganathan, C. N. Rao, *J. Mater. Chem.* **1997**, *7*, 2335–2337; b) D. P. Kim, C. L. Lin, T. Mihalisin, P. Heiney, M. M. Labes, *Chem. Mater.* **1991**, *3*, 686–692; c) J. Liu, R. Czerw, D. L. Carroll, *J. Mater. Res.* **2005**, *20*, 538–543.
- [10] L. J. Zhi, T. Gorelik, R. Friedlein, J. S. Wu, U. Kolb, W. R. Salaneck, K. Mullen, *Small* **2005**, *1*, 798–801.
- [11] a) T. P. Fellinger, F. Hasché, P. Strasser, M. Antonietti, *J. Am. Chem. Soc.* **2012**, *134*, 4072–4075; b) Y. D. Xia, R. Mokaya, *Chem. Mater.* **2005**, *17*, 1553–1560; c) Y. D. Xia, R. Mokaya, *Adv. Mater.* **2004**, *16*, 1553–1558; d) A. Vinu, K. Ariga, T. Mori, T. Nakanishi, S. Hishita, D. Golberg, Y. Bando, *Adv. Mater.* **2005**, *17*, 1648–1652.
- [12] J. Wei, D. D. Zhou, Z. K. Sun, Y. H. Deng, Y. Y. Xia, D. Y. Zhao, *Adv. Funct. Mater.* **2013**, *23*, 2322–2328.
- [13] a) W. Chaikittisilp, K. Ariga, Y. Yamauchi, *J. Mater. Chem. A* **2013**, *1*, 14–19; b) B. Liu, H. Shioyama, T. Akit, Q. Xu, *J. Am. Chem. Soc.* **2008**, *130*, 5390–5391; c) H. L. Jiang, B. Liu, Y. Q. Lan, K. Kuratani, T. Akita, H. Shioyama, F. Q. Zong, Q. Xu, *J. Am. Chem. Soc.* **2011**, *133*, 11854–11857.
- [14] a) S. J. Yang, T. Kim, J. H. Im, Y. S. Kim, K. Lee, H. Jung, C. R. Park, *Chem. Mater.* **2012**, *24*, 464–470; b) N. L. Torad, M. Hu, Y. Kamachi, K. Takai, M. Imura, M. Naitoa, Y. Yamauchi, *Chem. Commun.* **2013**, *49*, 2521–2523; c) W. Chaikittisilp, M. Hu, H. J. Wang, H. S. Huang, T. Fujita, K. C. W. Wu, L. C. Chen, Y. Yamauchi, K. Ariga, *Chem. Commun.* **2012**, *48*, 7259–7261; d) S. Lim, K. Suh, Y. Kim, M. Y. Yoon, H. Park, D. N. Dybtsev, K. Kim, *Chem. Commun.* **2012**, *48*, 7447–7449; e) H. B. Aiyappa, P. Pachfule, R. Banerjee, S. Kurungot, *Cryst. Growth Des.* **2013**, *13*, 4195–4199; f) N. L. Torad, M. Hu, S. Ishihara, H. Sukegawa, A. A. Belik, M. Imura, K. Ariga, Y. Sakka, Y. Yamauchi, *Small* **2014**, *10*, 2096–2107; g) N. L. Torad, R. R. Salunkhe,

- Y. Li, H. Hamoudi, M. Imura, Y. Sakka, C. C. Hu, Y. Yamauchi, *Chem. Eur. J.* **2014**, *20*, 7895–7900.
- [15] Y. Yang, Y. Zhang, C. J. Sun, X. S. Li, W. Zhang, X. H. Ma, Y. Ren, X. Zhang, *ChemCatChem* **2014**, *6*, 3084–3090.
- [16] B. P. Buffin, A. Kundu, *Inorg. Chem. Commun.* **2003**, *6*, 680–684.
- [17] P. P. Su, H. Xiao, J. Zhao, Y. Yao, Z. G. Shao, C. Li, Q. H. Yang, *Chem. Sci.* **2013**, *4*, 2941–2946.
- [18] X. Huang, X. P. Liao, B. Shi, *Green Chem.* **2011**, *13*, 2801–2805.
- [19] a) Z. D. Pozun, S. E. Rodenbusch, E. Keller, K. Tran, W. J. Tang, K. J. Stevenson, G. Henkelman, *J. Phys. Chem. A J. Phys. Chem. B J. Phys. Chem. C* **2013**, *117*, 7598–7604; b) Y. Y. Lin, Y. Qiao, Y. J. Wang, Y. Yan, J. B. Huang, *J. Mater. Chem.* **2012**, *22*, 18314–18320; c) Y. Yang, Y. Ren, C. J. Sun, S. J. Hao, *Green Chem.* **2014**, *16*, 2273–2280.
- [20] S. Gazi, R. Ananthkrishnan, *Appl. Catal. B* **2011**, *105*, 317–325.
- [21] X. K. Kong, Z. Y. Sun, M. Chen, C. L. Chen, Q. W. Chen, *Energy Environ. Sci.* **2013**, *6*, 3260–3266.
- [22] Y. H. Deng, Y. Cai, Z. K. Sun, J. Liu, C. Liu, J. Wei, W. Li, C. Liu, Y. Wang, D. Y. Zhao, *J. Am. Chem. Soc.* **2010**, *132*, 8466–8473.
- [23] a) S. Panigrahi, S. Basu, S. Praharaj, S. Pande, S. Jana, A. Pal, S. K. Ghosh, T. Pal, *J. Phys. Chem. C* **2007**, *111*, 4596–4605; b) P. Veerakumar, M. Velayudham, K. L. Lu, S. Rajagopal, *Appl. Catal. A* **2012**, *439–440*, 197–205; c) S. Wunder, F. Polzer, Y. Lu, Y. Mei, M. Ballauff, *J. Phys. Chem. C* **2010**, *114*, 8814–8820; d) H. Li, J. Liao, Y. Du, T. You, W. Liao, L. Wen, *Chem. Commun.* **2013**, *49*, 1768–1770.
- [24] A. Corma, *Chem. Rev.* **1997**, *97*, 2373–2420.
- [25] C. S. Kong, D. Y. Kim, H. K. Lee, Y. G. Shul, T. H. Lee, *J. Power Sources* **2002**, *108*, 185–191.
- [26] H. L. Peng, Z. Y. Mo, S. J. Liao, H. G. Liang, L. J. Yang, F. Luo, H. Y. Song, Y. L. Zhong, B. Q. Zhang, *Sci. Rep.* **2013**, 1765.

Received: July 21, 2015

Published online on September 23, 2015